ICEMG 2023-XXXXX

Performance Comparison of Predictive Functional Speed Controller Based on Extended State and Sliding Mode Disturbance Observers

Ahmadreza Karami-Shahnani[1], Mohammad Shokrani[2], Karim Abbaszadeh[3], Mohammad Farahzadi[4], Reza Nasiri-Zarandi[5]

[1]Department of Electrical Engineering, K.N.Toosi University of Technology, Tehran, Iran; ar.karami@email.kntu.ac.ir
[2]Department of Electrical Engineering, K.N.Toosi University of Technology, Tehran, Iran; mohammad.shokrani@email.kntu.ac.ir
[3]Department of Electrical Engineering, K.N.Toosi University of Technology, Tehran, Iran; abbaszadeh@kntu.ac.ir
[4] Faculty of Electrical Engineering, University of Science and Culture, Tehran, Iran; m.farahzadi@usc.ac.ir
[5] Electrical Machine Research Department, Niroo Research Institute (NRI), Tehran, Iran; rnasirizarandi@nri.ac.ir

Abstract

This work discusses the performance of the predictive functional control (PFC) approach by utilizing two well-known observers as disturbance estimators for permanent magnet synchronous motors (PMSMs), which are frequently characterized by nonlinearity and uncertainty. PFC serves as a link between complicated model predictive control (MPC) and PI(D)-based control. PFC is a simplified MPC that uses prediction and can be utilized with simple software and inexpensive hardware. It should be highlighted that the traditional PFC technique does not produce good results in the presence of significant disturbances. The disturbance can be instantly rejected by compensating current through a feedforward loop. To this end, some observers were introduced. The extended state observer (ESO) and sliding-mode observer (SMO) are promising candidates among different observers. In this work, the observers assess the controlled plant's lumped disturbance, and state feedback is used to achieve appropriate control performance. Based on the simulation results, thorough comparisons are made to determine which option is preferable for the application.

Keywords: Extended state observer (ESO), performance comparison, predictive functional control (PFC), sliding mode observer (SMO), speed controller.

Introduction

Permanent magnet (PM) machines are mostly employed in industrial applications because of their powerful features, such as their high power density and wide speed control range [1]. However, the PMSM faces various internal and external disturbances in actual applications, making it extremely hard to identify the upper bound of the lumped disturbance [2]. Additionally, most advanced control methods must select significant control gains to provide effective control efforts to suppress the negative impacts of disturbance, which lead to anundesirable dynamic and steady-state performance in PMSM [3].

Model predictive control (MPC) is one of the most effective advanced control techniques for industrial applications [4]. MPC predicts the future behavior of the states using a dynamic plant model and chooses the subsequent control action by optimizing a performance target function or an operating cost function at each sampling time [5, 6]. The well-known shortcoming of the MPC approach is that it requires a complex optimization problem to be solved at each sampling time to calculate the control actions, which leads to a heavy computational load. However, these controllers can be developed for dynamical systems thanks to the improved development of computer technology and the convex optimization technique [7]. In industry, proportional-integral-derivative (PID) control is well known. However, The PID parameters are difficult to adjust, and their use is limited by dead times.

Predictive functional control (PFC) provides excellent robustness, good tracking performance, and minimal online computing, making it suitable for controlling the speed of a linear motor. The prediction error of the PFC increases with higher external disturbance, which decreases the system's control precision [8, 9]. Although the predictive controller can asymptotically suppress disturbances through feedback regulation slowly, it is difficult to expect it without any penalization item directly relating to disturbance rejection ability in the cost function [6]. In the literature, various disturbance estimating methods have been presented [4]–[6]. Observer-based controllers have become one of the most often utilized strategies in industrial applications due to their significant ability in nonlinear control theory. The Extended state observer (ESO) is developed to estimate the state variable of the system and the external disturbance. ESO is used for the estimation of the state as well as disturbance [10]. The SMO is used to detect and compensate for the system's disturbances, helping the linear motor system to work better under control [11]. In [12], ESO is utilized for the PMSM speed controller disturbance estimate, and the disturbance rejection approach is applied. In [6], a PFC is added to ESO in order to enhance PMSM control performance. In [13], for speed regulation of PMSM, model reference adaptive control with disturbance estimate using ESO is developed. In [14], the terminal sliding mode control approach controls PMSM. To improve the tracking performance of the PMSM drive system with various types of disturbance, a traditional first-order SMC approach based on ESO was developed in [15].

This paper investigates the performance of a PFC speed controller based on ESO and SMO disturbance observer. The comprehensive comparison between observers in terms of implementation, tuning, running effort, and overall system performance is performed to

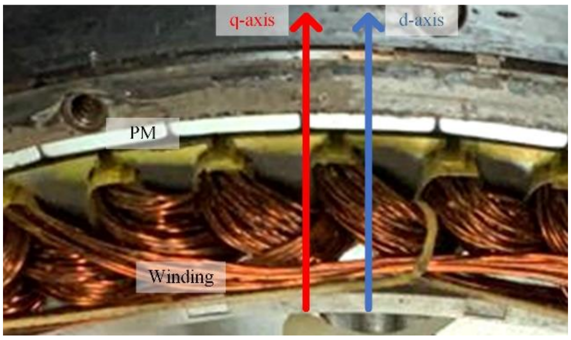

Figure 1. Structure of SPMSM with rotor *dq*-axis

select the best construction for an anti-disturbance speed controller based on predictive functional control. To this end, the dynamic model of the surface permanent magnet synchronous motor (SPMSM) in the Laplace domain is developed in Section II. The outline and design of PFC with disturbance observer based on ESO and SMO are presented in Section III. Section IV provides the simulation results to investigate the performance comparison, followed by conclusions in Section V.

Laplace Domain Dynamic Model

The structure of the 46-pole BLDCM used in this work is depicted in Figure 1. The *d*- and *q*- axes are also shown in this Figure. The SPMSM is described in the rotor *dq*-reference frame (RRF) using the following equations. Also, as seen in Figure 1, PMs are aligned with the *d*-axis in this modeling. The following is a possible form for the flux linkage equations.

$$\lambda_d = L_d i_d + \Lambda_{PM} \tag{1}$$

$$\lambda_q = L_q i_q \tag{2}$$

Here, $\lambda_{d,q}$, $L_{d,q,}$ and $i_{d,q}$ are flux linkages, inductance, and currents related to the *d*- and *q*-axes, respectively. The PM-flux linkage is also a constant value shown by the Λ_{PM}. The voltage equations in RRF can be calculated as follows:

$$V_d = R_s i_d + \rho(L_d i_d + \Lambda_{PM}) - \frac{P}{2}\omega_r (L_q i_q) \tag{3}$$

$$V_q = R_s i_q + \rho(L_q i_q) + \frac{P}{2}\omega_r (L_d i_d + \Lambda_{PM}) \tag{4}$$

$V_{q,d}$, R_s, P, ρ, and ω_r are voltage in the *dq* RRF, stator resistance, number of poles, time derivative, and mechanical speed, respectively. In (3) and (4), the $\omega_e = \frac{P}{2}\omega_r$ which is known as electrical speed. By rewriting (3) and (4), the currents in RRF can be calculated as follows:

$$i_d = \frac{1}{L_d}\int V_d - R_s i_d + \omega_e (L_q i_q) \tag{5}$$

$$i_q = \frac{1}{L_q}\int V_q - R_s i_q - \omega_e (L_d i_d) - \omega_e \Lambda_{PM} \tag{6}$$

The average torque can be determined when iron saturation and torque fluctuations are not considered.

$$\tau_{em} = \frac{3}{4} P i_q ((L_d - L_q) i_d + \Lambda_{PM}) \tag{7}$$

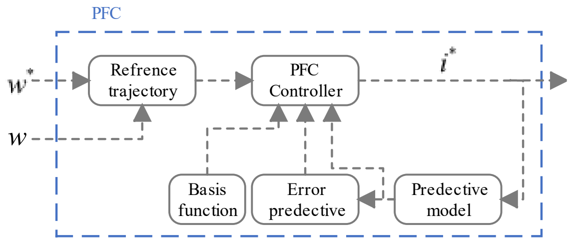

Figure 2. The schematic of conventional PFC

Here, τ_{em} is the electromagnetic average torque. In (7), the first and second terms are the torque components produced by PMs and reluctance, respectively. As it is well-known, in the case of SPM arrangements $L_d = L_q = L$. These assumptions determine the simplified electromagnetic torque as (8).

$$\tau_{em} = \frac{3}{4} P i_q \Lambda_{PM} = k_t \Lambda_{PM} \tag{8}$$

Where k_t is called the torque constant. As seen in (8), only i_q produces the torque. Therefore, the i_d is adjusted to 0 in the control of SPMSM. Additionally, speed can be obtained using the general dynamic equation for electrical machines.

$$\omega_r = \frac{1}{J}\int (\tau_{em} - \tau_L - \tau_d - B\omega_r) \tag{9}$$

In (9), J, B, τ_L, and τ_d represent the total inertia of the system, viscous friction coefficient, load torque, and dry friction with other unknown uncertainties.

According to (1) to (9), the dynamic model of the motor is nonlinear and includes product terms of state variables, such as motor speed ω_e, with the current i_d or i_q. To facilitate online implementation, a linear model is utilized. Because the speed loop's dynamics change more sluggish than the current loop's, the gain of current loop control can be assumed as 1 in the modeling stage. The disparity between the actual current (i_q) and the commanded current (i_q^*), which includes the dynamic of the current loop, is afterward regarded as a disturbance. By these assumptions and (8), and (9), a first-order model of the mechanical dynamics of a SPMSM can be presented in the Laplace domain as (10).

$$\Omega(s) = \frac{k_t i_q}{Js + B} - \frac{\tau_L + \tau_d}{Js + B} \tag{10}$$

Predictive Functional Control

The PFC method's primary design processes for the SPMSM speed loop are introduced in this section. The third generation of predictive control is known as PFC. It has three characteristics common to predictive control techniques, i.e., predictive model, cost function, and feedback correction. The block diagram of conventional PFC is depicted in Figure 2. As seen in this Figure, the PFC speed controller has four parts which are explained in the following.

The PFC method's control input u is a linear combination of base functions. The desired controlled variable's form can determine how the base function is used.

$$u(k+i)=\sum_{j=1}^{N} w_j f_j(i), \quad i=1,2,\ldots,H \qquad (11)$$

Where N *is* the number of base functions, w_j is the optimized coefficients from the optimized cost function, k is the sample time, H is the optimization horizon, and f_j is the value of the base function. Typically, basic functions consist of canonical functions like step, ramp, parabola, etc. The nature of base functions depends on the reference signal type. The output of the speed controller, i.e., i_q, serves as the predictive function control quantity in the linear SPMSM. This allows the step function to be used as the base function for speed control objectives.

The plant's future outputs are predicted online over a defined finite horizon using a linear numerical model. As mentioned before, PFC does not perform a fast and satisfactory response in terms of disturbance compensation. Therefore, the second term in (10) that serves as a disturbance is disregarded at this design stage. For PFC design, a discrete-time model is required. A discrete-time model is presented in (12) by forward Euler discretizing.

$$\begin{aligned}&\omega_m(k+i|\ k)=\left(e^{-\frac{T_S B}{J}}\right)^i \omega_m(k)\\&+\frac{k_t}{B}\left(1-\left(e^{-\frac{T_S B}{J}}\right)^i\right)i_q^*(k)\end{aligned} \qquad (12)$$

In (12), T_s is the sample time and $\omega_m(k+i)$ is the model's output prediction at the (k+1)th sampling time.

Due to linear model mismatch, various noise, and other uncertainties, there are some discrepancies between the predicted model output and the actual result. The error is defined as (13).

$$e(k+(H-1))=\ldots=e(k)=\omega_{real}(k)-\omega_m(k) \qquad (13)$$

Here, ω_{real}(k) is the actual output of the system in $t=kT_s$.

A reference trajectory creates a smooth transition to the target trajectory or set point within a specific future time frame. To depict the reference trajectory, a reference model is offered. The primary goal of the suggested approach is to find a control rule that facilitates the controlled signal to follow the reference trajectory. In this work, the reference trajectory is a first-order exponential which is presented in (14).

$$\begin{aligned}&\omega_r(k+i)=\omega^*(k+i)\\&-\left(e^{-\frac{T_S}{T_r}}\right)^i\left[\omega^*(k)-\omega(k)\right]\end{aligned} \qquad (14)$$

In (14), ω_r, $\omega*$, and T_r are reference trajectory, setpoint value, and the desired closed-loop response time.

Future control values are determined by decreasing the sum of squared tracking errors and a penalty on the control input as calculated in (15). The system's output will converge to the reference trajectory thanks to the cost function extracted below.

$$\begin{aligned}&\min J_H=\sum_{i=1}^{H}\left[\omega_r(k+i)-\omega_m(k+i)-e(k+i)\right]^2\\&+r^2 i_q^{*2}(k)\end{aligned} \qquad (15)$$

Since the model in (10) is linear, it is possible to algebraically determine the minimum value of the cost function in (15). The matrices in (15) must be updated at each sampling time. Then, the controller is developed by putting $\partial J/\partial i_q^*=0$, as calculated in (16).

$$i_q^*=\left(W_b^T Q W_b+R\right)^{-1} W_b^T Q\left[W_r(k)-W_o(k)-E(k)\right]$$

$$where\begin{cases}W_r(k)_{(H\times 1)}=\left[\omega_r(k+1)\ldots\omega_r(k+H)\right]^T;\\E(k)_{(H\times 1)}=[e(k+1)\ldots e(k+H)]^T;\\Q_{(H\times H)}=\operatorname{diag}\left[q_1^2\ldots q_H^2\right];\\R_{(1\times 1)}=r^2;\end{cases}$$

(16)

Here, r is the weight for the control efforts of the inputs, and q is a parameter that permits emphasis on each controlled output and its predictions.

Lumped Disturbance Modeling

In order to improve the disturbance rejection performance, a feedforward compensation section is added to the PFC in addition to the feedback part. Although it is not considered during the PFC design stage, the tracking error of the q-axis current loop is considered as a disturbance component. Uncertainties, friction, and external load are additional components of disturbance. The dynamic motor equation from (10) can be rewritten as:

$$\begin{aligned}\dot{\omega}&=\frac{k_t}{J}i_q-\frac{B}{J}\omega-\frac{\tau_L+\tau_D}{J}\\&=\frac{k_t}{J}i_q^*-\left(\frac{B}{J}\omega+\frac{\tau_L}{J}+\frac{\tau_D}{J}+\frac{k_t}{J}\left(i_q^*-i_q\right)\right)\\&=\frac{k_t}{J}i_q^*+D(t)=\frac{k_t}{J}i_q^{*\prime}\end{aligned} \qquad (17)$$

In (17), *D(t)* can be considered as the lumped disturbances.

Sliding Mode Disturbance Observer

SMO can be utilized as a disturbance estimation technique for the SPMSM. The form of the sliding mode observer is depicted in (18) for the system of (17) with various disturbances.

$$\begin{cases}\dot{\hat{\omega}}(t)=k_t i_q(t)+\xi(t)\\\xi(t)=\eta\operatorname{sign}(\sigma)\end{cases} \qquad (18)$$

The observer error can be calculated as follows:

$$\sigma(t)=\omega(t)-\hat{\omega}(t) \qquad (19)$$

Where the *hat* sign represents the estimated variable. Also, the parameters in (18) are depicted in Figure 3. The bounded condition is satisfied by the disturbance magnitude.

$$\eta>|D(t)| \qquad (20)$$

By subtracting (18) from (16), it can be obtained as:

$$M\dot{\sigma}(t)=-D(t)-\eta\operatorname{sign}(\sigma) \qquad (21)$$

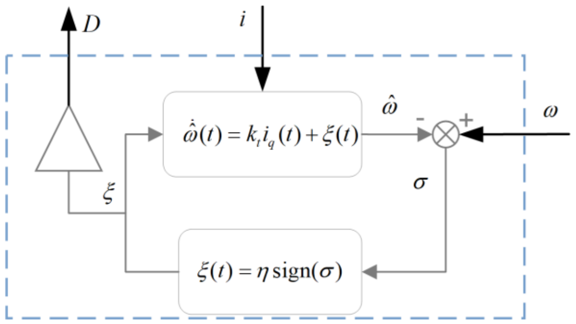

Figure 3. The block diagram of SMO

The Lyapunov function can be defined as (22).

$$V(t)=\frac{1}{2}M\sigma^2(t) \tag{22}$$

By combining with the bounded conditional of (20), the derivation is obtained as:

$$\begin{aligned}\dot{V}(t)&=M\dot{\sigma}(t)\sigma(t)\\&=\sigma(t)(-D(t)-\eta\,\mathrm{sign}(\sigma))<0\end{aligned} \tag{23}$$

The $\sigma(t)$ can asymptotically converge to zero because Lyapunov is a negative definite function. According to (18) and (23), the disturbance can be obtained as follows:

$$D(t)=-\xi(t) \tag{24}$$

Finally, according to (17) and (24), the compensated desired current can be calculated as (25).

$$i_q^{*\prime}=i_q^*+\frac{J}{k_t}D(t) \tag{25}$$

In (25), the first term is calculated from PFC, and the second is from achieved SMO.

Extended State Disturbance Observer

As indicated, a feedforward control scheme is considered to compensate the disturbances. An uncertain nonlinear function with constrained unknown external disturbance which is presented in (26), is assumed as system.

$$y^{(n)}=g\left(y,\dot{y},\ldots,y^{(n-1)},k\right)+d(k)+b_0u \tag{26}$$

Where g is an unknown function. Generally, (n+1)-order ESO is utilized for the n-order system. The ESO uses only the measured output of the system, which can be described as (27).

$$\begin{cases}\varepsilon_0=z_1(k)-y(k)\\ z_1(k+1)=z_1(k)+h\left(z_2(k)-\beta_1\varepsilon_0\right)\\ z_2(k+1)=z_2(k)+h\left(z_3(k)-\beta_2\,fal\left(\varepsilon_0,\alpha_1,\delta_1\right)\right)\\ \vdots\\ z_n(k+1)=z_n(k)+h\left(z_{n+1}(k)-\beta_n\,fal\left(\varepsilon_0,\alpha_1,\delta_1\right)+b_0u(k)\right)\\ z_{n+1}(k+1)=z_{n+1}(k)-h\beta_{n+1}\,fal\left(\varepsilon_0,\alpha_2,\delta_1\right)\end{cases}$$

(27)

In (27), $z_1,z_2,\ldots,z_n$ are the estimate of states $y_1,y_2,\ldots,y_n$ and z_{n+1} is the estimated component of the unknown bounded disturbances. Also $\alpha_1,\alpha_2,\beta_1,\beta_2\ldots\beta_{n+1}$, and δ_1 are design parameters to be determined. The function $fal(\varepsilon,\alpha,\delta)$ can be defined as:

$$fal(\varepsilon,\alpha,\delta)=\begin{cases}|\varepsilon|^{\alpha}\,\mathrm{sgn}(\varepsilon), & |\varepsilon|>\delta\\ \dfrac{\varepsilon}{\delta^{1-\alpha}}, & |\varepsilon|\le\delta\end{cases} \tag{28}$$

We define $x_2=D(t)$, $x_1=\omega$, then (17) can be rewritten as the following state equation:

$$\begin{cases}\dot{x}_1=x_2+\dfrac{K_t}{J}i_q^*\\ \dot{x}_2=d(t)\end{cases} \tag{29}$$

Where *d(t)* is the variation rate of system uncertainty and disturbance, then, for system (29), the following second-order linear ESO can be created:

$$\begin{cases}\dot{z}_1=z_2-2\gamma\left(z_1-x_1\right)+b_0i_q^*\\ \dot{z}_2=-\gamma^2\left(z_1-x_1\right)\end{cases} \tag{30}$$

Where b_0 is an estimate of $\frac{k_t}{J}$, $-\gamma$ is the desired observer pole ($\gamma>0$), z_1 is an estimate of speed, and z_2 is an estimate of the lumped disturbances *D(t)*. The compensated desired current can be calculated as (31).

$$i_q^{*\prime}=i_q^*+\frac{z_2}{b_0} \tag{31}$$

In (31), the first term is achieved from PFC, and the second is calculated from ESO.

Simulation and Comparison

An SPMSM with a PFC speed controller and two disturbance observers have been simulated based on (1)-(31) to demonstrate the performance of the proposed disturbance observers. To have a fair comparison, both observers are utilized for the same system. The rated parameters of SPMSM, PFC speed controller, PI current controller, and observer parameters are presented in Table I.

The reference speed and load trajectories are depicted in Figure 4(a). The load is changed from no-load condition to 5 N.m at t=0.2 s and from 5 N.m to 10 N.m at t= 0.58 s. Also, the speed change at t=0.39 s from block rotor condition to 100 rpm and from 100 rpm to 200 rpm at t=0.75s. In this way, five intervals and operating points can be taken into account.

1- $0\le t<0.2$

In this interval, the SPMSM experience block rotor condition. As evident in Figure 4(c), observers do not produce any compensation current because there is no disturbance in the system. So, the compensated current is 0 A. The speed command is set to zero, so the output of the PFC speed controller is zero. Therefore, the total current which is expected in (25) estimated speed from both observers is depicted in Figure 4(e). The estimation of SMO has more fluctuations related to this observer's nature. However, both observers have the same average

Table 1. Rated Values for Simulation

	Parameters	Sym.	Unit	Value
SPMSM	Rated Power	P_n	W	250
	Rated Speed	n	rpm	170
	Number of Poles	N_p	-	46
	Battery Voltage	V_{DC}	V	36
	Phase Resistance	R_s	mΩ	110
	d-axis Inductance	L_d	mH	0.2
	q-axis Inductance	L_q	mH	0.2
	PM Flux Linkage	Λ_{PM}	V/Hz	0.141
	Moment of Inertia	J	Kg.m^2	0.0014
	Viscous Damping	B	$\frac{N.m.s}{rad}$	0.0004
PFC	Sample Time	T_s	μs	250
	Response Time	T_r	μs	50
	Prediction Length	H	-	6
	-	r	-	2
	-	Q	-	I_{6*6}
Current Controller	Proportional Gain	k_P	-	50
	Integral Gain	k_I	-	2500
ESO	-	δ_1	-	0.1
	-	α_1	-	0.9
	-	β_1	-	5×10^3
	-	β_2	-	5×10^4
SMO	-	ξ	-	17

value. Finally, the SPMSM output measured speed is depicted in Figure 4(f), and both methods can follow the commands successfully.

2- $0.2 \leq t < 0.4$

In this interval, the SPMSM experience dynamic brake condition. The load drives the motor while the motor command speed is zero. In this condition, the rotor must be blocked, and the load torque must be maintained simultaneously. As shown in Figure 4(b), observers estimate the disturbance related to the load torque. So, the observer produces the compensated current, as seen in Figure 4(c). Due to its nature, some fluctuation can be observed in the SMO's produced current. Figure 4(e) shows that at t=0.2, observers experienced a transient mainly due to motor transient speed depicted in Figure 4(f).

3- $0.4 \leq t < 0.6$

The SPMSM is in motor running mode throughout this interval. In this interval, the rotor must rotate at a specific speed while maintaining the load torque. As it is obvious in Figure 4(b), observers do not produce any compensation current because there is no disturbance in the system. The PFC speed controller maintains the current for speed change, and the current is forced to a minimum value according to the cost function. So, the compensated current is

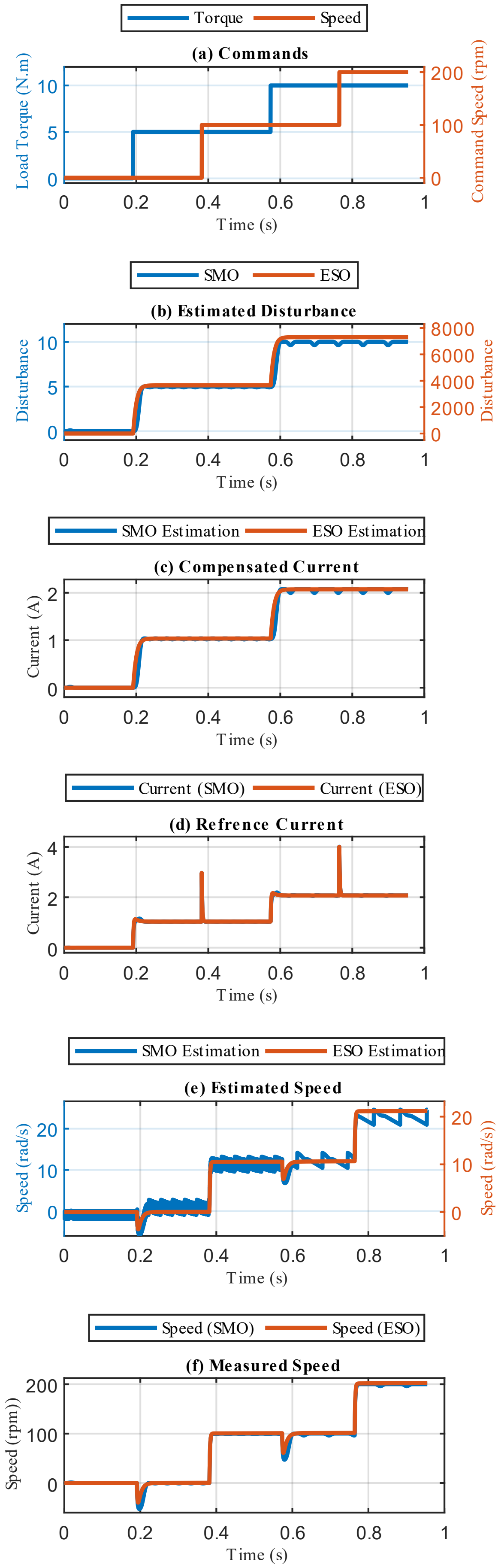

Figure 4. Simulation results.

produced by PFC, as seen in Figure 4(d). Figure 4(e) shows that observers followed the commanded speed successfully. Also, Figure 4(f) indicates that the SPMSM follows the desired values precisely.

4- $0.4 \le t < 0.6$

In this interval, the SPMSM works in motor mode. The load torque is changed at t=0.4, while the motor speed must be the same as the previous interval. The explanation is the same as what was mentioned for the second interval. Figure 4(f) shows that the SPMSM can follow the desired values precisely.

5- $0.6 \le t < 0.8$

The speed is increased to the rated value at t=0.6 . The explanation is the same as what was mentioned for the third interval. Figure 4(d) shows the performance of the PFC speed controller at this moment. Also, Figure 4(f) depicts the speed of SPMSM, which is adopted well with the desired value for both SMO and ESO disturbance observer.

For more comparisons, the transient behavior of the controller with SMO and ESO disturbance observer is illustrated in Figure 5. Figure 5(a) represents the performance of the disturbance observer because it is the speed transient manner of SPMSM when the load change suddenly. At t=0.4, the load increased. As shown in Figure 5(a), the ESO can keep the speed in a constant value with a lower undershoot value. The settling time is almost the same for both observers. Also, Figure 5(b) shows that the PFC speed controller based on the ESO can control the reference current (torque) more smoothly. However, the PFC speed controller based on SMO has acceptable performance.

Furthermore, at t=0.11, the speed changed suddenly. At this moment, any disturbance observer does not react because the speed tracking can be handled by the PFC speed controller and does not consider as a disturbance. Both control systems with SMO and ESO disturbance observers perform similarly under speed variations.

In terms of implementation, both observers have some parameters which should be designed by trial and error. As presented in Table I, the number of these uncalculated variables is more in ESO. Additionally, SMO utilizes a simpler error function than ESO, which facilitates implementation.

Conclusions

The comprehensive performance comparison for a speed controller based on a predictive functional control method and sliding mode and extended state observer as disturbance observer is performed in this paper. The dynamic speed equation in the Laplace domine is extracted. Then the guidelines for designing a speed controller based on PFC are presented, and the lumped disturbance is determined in the speed equation. Also, a sliding mode and extended state observer are developed for fast and precise disturbance rejection. The comparison study was performed for a 250 W SPMSM which is utilized in a scooter propulsion system. The results showed that a speed controller based on a predictive functional control method could track the speed reference adequately. In the same way, the disturbance can

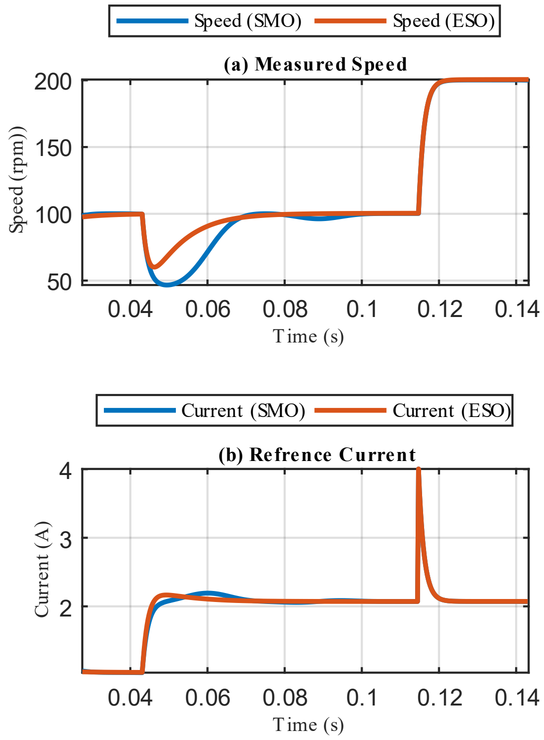

Figure 5. Transient behavior of PFC speed controller base on SMO and ESO disturbance observer.

compensate by sliding mode or extended state observer as well as possible. However, the disturbance observer based on extended state observer had better performance regarding over/undershoot and smooth tracking. On the other hand, the disturbance observer based on the sliding mode observer benefited from the lower computational effort.

References

[1] R. Nasiri-Zarandi, A. Karami-Shahnani, M. S. Toulabi and A. Tessarolo, "Design and Experimental Performance Assessment of an Outer Rotor PM Assisted SynRM for the Electric Bike Propulsion," in *IEEE Transactions on Transportation Electrification*, 2022, doi: 10.1109/TTE.2022.3202819.

[2] Q. Hou and S. Ding, "Finite-Time Extended State Observer-Based Super-Twisting Sliding Mode Controller for PMSM Drives With Inertia Identification," *in IEEE Transactions on Transportation Electrification*, vol. 8, no. 2, pp. 1918-1929, June 2022.

[3] G. Zhang, G. Wang, B. Yuan, R. Liu, and D. Xu, "Active disturbance rejection control strategy for signal injection-based sensorless IPMSM drives," *IEEE Trans. Transport. Electrific.*, vol. 4, no. 1, pp. 330–339, Mar. 2018.

[4] J. M. Maciejowski, "*Predictive Control With Constraints.*" London, U.K.: Prentice-Hall, Jun. 2001.

[5] W. H. Chen, D. J. Ballance, and P. J. Gawthrop, "Optimal control of nonlinear systems: A predictive

control approach," *Automatica*, vol. 39, no. 4, pp. 633–641, Apr. 2003.

[6] C. Line, C. Manzie, and M. C. Good, "Electromechanical brake modeling and control: From PI to MPC," *IEEE Trans. Control Syst. Technol.*, vol. 16, no. 3, pp. 446–457, May 2008.

[7] H. Liu and S. Li, "Speed Control for PMSM Servo System Using Predictive Functional Control and Extended State Observer," *in IEEE Transactions on Industrial Electronics*, vol. 59, no. 2, pp. 1171-1183, Feb. 2012.

[8] Z. Lei, L. Jian and H. Jia-cai, "Research on predictive functional control based on disturbance observer for PMLSM speed system," *2017 36th Chinese Control Conference (CCC)*, 2017, pp. 4650-4653.

[9] J. Lin et al., "Predictive Functional Control Based on Sliding Mode Observer for Linear Motor Speed System," *2018 5th International Conference on Information Science and Control Engineering (ICISCE)*, 2018, pp. 895-899.

[10] A. Apte, V. A. Joshi, H. Mehta and R. Walambe, "Disturbance-Observer-Based Sensorless Control of PMSM Using Integral State Feedback Controller," *in IEEE Transactions on Power Electronics*, vol. 35, no. 6, pp. 6082-6090, June 2020.

[11] J. Lin et al., "Predictive Functional Control Based on Sliding Mode Observer for Linear Motor Speed System," *2018 5th International Conference on Information Science and Control Engineering (ICISCE)*, 2018, pp. 895-899.

[12] S. Li, H. Liu, and S. Ding, "A speed control for a PMSM using finite time feedback control and disturbance compensation," *Transaction of the Institute of Measurement and Control*, vol. 32, no. 2, pp. 170–187, 2010.

[13] S. Li, H. Liu, and W. Fu, "An improved predictive functional control method with application to pmsm systems," *International Journal of Electronics*, vol. 104, no. 1, pp. 126–142, 2017.

[14] S. Li, M. Zhou, and X. Yu, "Design and implementation of terminal sliding mode control method for PMSM speed regulation system," *IEEE Transactions on Industrial Informatics*, vol. 9, no. 4, pp. 1879–1891, November 2013.

[15] L. Qu, W. Qiao, and L. Qu, "An extended-state-observer-based sliding mode speed control for permanent-magnet synchronous motors," *IEEE J. Emerg. Sel. Topics Power Electron.*, vol. 9, no. 2, pp. 1605–1613, Apr. 2021.